UNIVERSITY OF LJUBLJANA

FACULTY OF MATHEMATICS AND PHYSICS

Seminar

Photonic crystal fibers

Author: Peter Jakopič
Mentor: Prof. dr. Irena Drevenšek Olenik

May 2008

Abstract

Photonic crystal fibers (PCF) are promising novel technology with several possible applications in wave guides, nonlinear optics, fiber lasers, sensory systems, etc. The photonic bandgap structure of a simple 1D photonic lattice is derived and comparison between dispersion relations of standard optical fiber and microstructured fiber is presented. Few most common PCF designs are reviewed and compared to standard glass fibers. The main application aspects are reviewed.

Contents

1 Introduction

Until early 1996, an optical fiber was a solid thread surrounded by another material with a lower refractive index. With the discovery of photonic crystals, new alternative have been suggested and thoroughly studied. Photonic crystal fibers (PCF) [1] - fibers with a periodic transverse microstructure - present today a wide research area and many innovative optical devices based on PCFs have emerged. PCFs operation is based on specific behavior of optical modes in the microstructure of fiber cladding, which yields band structure of modes, similar to the band structure of electrons in a periodic potential. PCFs have extended the range of possibilities in optical fibers, both, by improving well-established properties and introducing new features, such as low-loss guidance in a hollow core. In the second section we briefly review the standard optical fiber and its characteristics. The basic mechanism of PCF light guidance and its comparison with standard fibers is given in the third section. In the fourth section various types of PCFs are described and in the fifth one, main applications categories are presented.

2 Standard optical fibers

In standard optical fibers light is guided by total internal reflection on the interface between high refractive index core and low refractive index cladding. (Fig. 1)

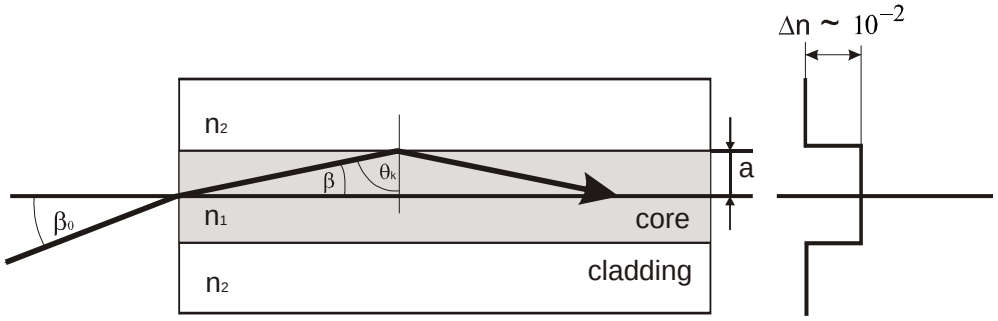

Figure 1: Schematic drawing of a standard - "step index" optical fiber. The core with higher refractive index is surrounded by the cladding with lower refractive index. Light guidance can be explained by ray optics considering total internal reflection on core/cladding interface.

The most typical material for fabrication of standard fibers is quartz glass (fused silica), which has the refractive index of approx. 1.457. The difference between core and cladding is achieved by addition of dopants, such as Germanium, which increase the refractive index for approx 1×10^{-2}. The above described geometric picture cannot explain all optical properties of fibers, to explain some of them one must solve the Maxwell equations for inhomogeneous dielectric medium. We add Maxwell equations up to obtain Helmholtz equations:

$$\boldsymbol{\nabla}^2\mathbf{E}\left(\mathbf{r},z,t\right) - \frac{n_i^2}{c^2}\frac{\partial^2\mathbf{E}\left(\mathbf{r},z,t\right)}{\partial t^2} = 0 \quad \text{and} \quad \boldsymbol{\nabla}^2\mathbf{H}\left(\mathbf{r},z,t\right) - \frac{n_i^2}{c^2}\frac{\partial^2\mathbf{H}\left(\mathbf{r},z,t\right)}{\partial t^2} = 0, \tag{1}$$

where n_i are refractive indices of a dielectric medium i. Then we separate temporal behavior using:

$$\mathbf{E}\left(\mathbf{r},z,t\right) = E\left(\mathbf{r},z\right)\exp\left(-i\omega t\right) \quad \text{and} \quad \mathbf{H}\left(\mathbf{r},z,t\right) = \mathbf{H}\left(\mathbf{r},z\right)\exp\left(-i\omega t\right), \tag{2}$$

where ω is light frequency, $\mathbf{r}$ is radial vector from axis center and z is longitudinal coordinate. Eqs. 1 thus yield:

$$\boldsymbol{\nabla}^2\mathbf{E}\left(\mathbf{r},z\right) + k_i^2\mathbf{E}\left(\mathbf{r},z\right) = 0 \quad \text{and} \quad \boldsymbol{\nabla}^2\mathbf{H}\left(\mathbf{r},z\right) + k_i^2\mathbf{H}\left(\mathbf{r},z\right) = 0, \tag{3}$$

where $k_i = \frac{n_i\omega}{c} = \frac{2\pi}{\lambda}$ and λ is wavelength of light in vacuum. In optical fiber we seek for propagating solutions:

$$\mathbf{E}\left(\mathbf{r},z\right) = \mathbf{E}\left(\mathbf{r}\right)\exp\left(i\beta z\right) \quad \text{and } \mathbf{H}\left(\mathbf{r},z\right) = \mathbf{H}\left(\mathbf{r}\right)\exp\left(i\beta z\right), \tag{4}$$

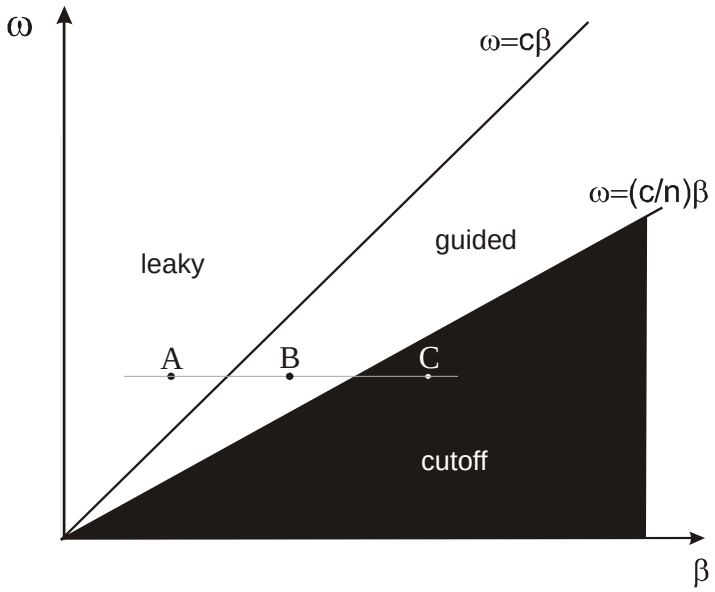

Figure 2: Propagation diagram for step index profile, where outside layer is air. Above the light line (dispersion relation for light in free space) for vacuum (point A) only leaky modes exist, i.e. light is not guided along fiber. In region between light line for silica and light line for air (point B), light is trapped inside silica by total internal reflection (guided modes). In the region below light line for silica, no oscillating solutions are found (cutoff area). [3]

where β is longitudinal wave vector in the axis direction. Substituting Eqs. 4 in Eqs. 3 we get:

$$\nabla_{\perp}^2 \mathbf{E}(\mathbf{r}) + \left(k_i^2 - \beta^2\right)\mathbf{E}(\mathbf{r}) = 0 \quad \text{and} \quad \nabla_{\perp}^2 \mathbf{H}(\mathbf{r},z) + \left(k_i^2 - \beta^2\right)\mathbf{H}(\mathbf{r},z) = 0. \tag{5}$$

According to Eq. 5, when the value of the parameter $k_i^2 - \beta^2$ (often called transverse wave vector) is positive, oscillating solutions can be found within a layer and when it is negative, only evanescent solutions are possible. Therefore, when for specific layer holds:

$$\omega > \frac{c}{n_i}\beta, \tag{6}$$

light can be introduced into this layer, in the opposite case the light is totally reflected from the interface (i.e. only evanescent wave extends to interior). The limit situation, when $\omega = (c/n_i)\,\beta$, is called a light line for the layer [3]. If we consider ray optics, this is the case, in which the ray is parallel to the symmetry axis of the layers. In Fig. 2, the propagation diagram for simplified waveguide (silica rod surrounded by air) is presented. In the region above light line for air (point A) an oscillating solution in both - silica and air layers exists therefore light is freely passing silica-air interface and is not guided. These solutions are called leaky modes. In the region above light line for silica and below light line for air (point B), solutions are oscillating in silica and evanescent in air, therefore light is trapped inside silica layer and therefore these solutions are called guided modes (or just modes). Below the light line for silica, only evanescent solutions are found (cut-off modes), i.e. light can't be introduced to any of layers.

According to the discussion above, propagation constant β of the guided modes in step-index optical fiber ranges from

$$\frac{\omega n_2}{c} < \beta < \frac{\omega n_1}{c}, \tag{7}$$

where n_1 and n_2 are refractive indices of the core and cladding, respectively. The cladding is usually surrounded by polymer with higher refractive index and high attenuation to suppress oscillations in cladding. Same as with electrons, photons can tunnel through cladding layer to a polymer coating, therefore sufficient thickness of the cladding is required to prevent power loss.

Eq. 5 is solved in cylindrical coordinates and boundary conditions on the core/cladding interface are applied [2]. Some of the solutions are displayed on Fig. 3.

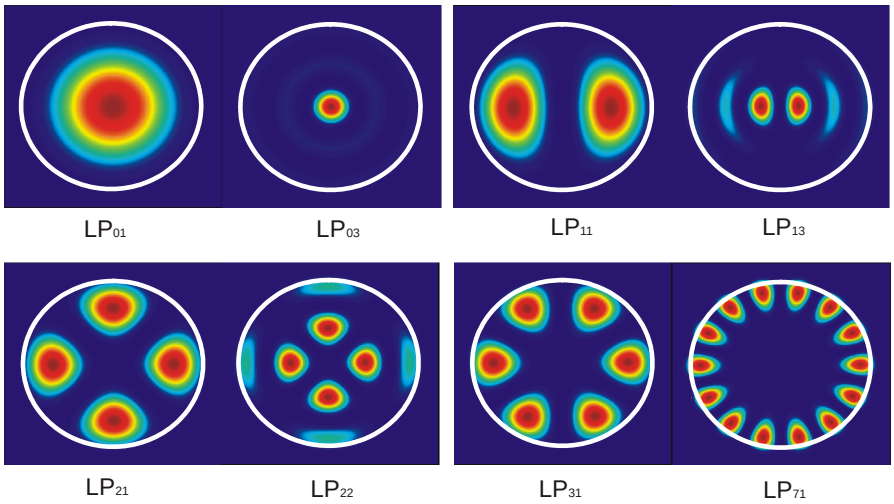

Figure 3: Transverse profile of light intensity for some basic modes in cylindrical optical fiber. LP_{01} is the fundamental mode, which is always present. White line presents core/cladding interface. It can be seen that higher order modes are less confined to the center of the core, so they experience lower effective refractive index, since a significant part of the field is extended into lower index cladding. This gives rise to modal dispersion, which is one of the most limiting factors of signal distortions in multimode fibers.

The first mode exist for any step-index configuration and wavelength, others exist only below cut-off wavelength λ_c which is determined by the equation

$$\frac{2\pi a}{\lambda_c}\sqrt{(n_1^2 - n_2^2)} = 2.405, \tag{8}$$

where a is the core diameter. Fibers in which only the fundamental mode is propagating are called single-mode fibers. Typical dimensions of such fibers are $8\,\mu$m and $125\,\mu$m for core and cladding, respectively.

Among the parameters that characterize the quality of optical fibers we will mention the most important ones: numerical aperture, optical attenuation and dispersion coefficient. Numerical aperture is the sine of the maximum angle at which the incident light is still guided inside core. It is easy to show, that:

$$NA = \sqrt{n_1^2 - n_2^2}\,. \tag{9}$$

Optical attenuation is defined as

$$A[dB/km] = \frac{1}{L} 10 * \log\left(\frac{P_{in}}{P_{out}}\right), \tag{10}$$

where L is length of optical fiber and P_{in} and P_{out} are incident and output optical powers. Typical values in single mode optical fiber, which is used for telecommunications, are: $A_{@1310} = 0.35$ dB/km and $A_{@1550} = 0.19$ dB/km where indices denote typical communicating wavelengths. At this wavelengths light can be guided at distance of approx 100 km with no amplification. Attenuation in optical fibers appears manly due to Rayleigh scattering, ultraviolet absorption at short wavelengths (< 400 nm) and infrared absorption at long wavelengths (>1650 nm). Another limiting effect are waveguide imperfections, i.e. deviations from step-index profile, and bend loss, which is due to fiber bending. The group velocity dispersion (GVD) is another limiting property of optical fibers and refers to spreading of a light pulse due to slightly different propagation velocity of different modes

(modal dispersion) or fields of different wavelengths (waveguide and material dispersion). In single mode fibers, there is no modal dispersion, while waveguide and material dispersion cancel each other at zero-dispersion-wavelength (ZDW). This is for silica step-index profile typically around 1310 nm. The GVD in SM fibers is measured by dispersion coefficient given in ps/ nm km and typically ranges from about -10 ps/ nm km at 1.2 μm to 15 ps/ nm km at 1.6 μm.

3 Light propagation in periodic dielectric media

A periodic variation of dielectric constant in the fiber cladding is one of the main characteristics of PCFs. In this chapter we will describe the solutions of Maxwell's equations in a simple 1D photonic crystal as an illustrative example of light behavior in periodic media. In PCF, however, the calculation is much more complicated and numerical methods have been developed to obtain field modes for various types of PCFs [4]. The dispersion relation, introduced in Fig 2, is drastically changed in periodic media. One of the most significant new properties are bandgaps, which have strong similarity with bandgaps of electron energy in the periodic potential. The occurrence of photonic bandgaps can be derived by solving the Maxwell's equations using the Bloch's theorem. Let us consider two kinds of dielectric layers A and B of the same width $a/2$ alternating in the z direction, as shown in Fig. 4. For the purpose of simplicity we will use scalar wave equation for

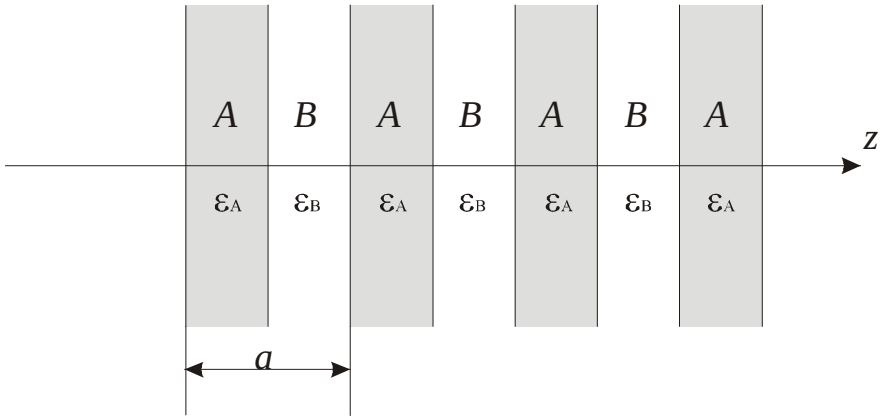

Figure 4: One-dimensional stack of A and B films in the z direction. The length of unit cell a defines the periodicity of this 1D photonic crystal.

the electric field in z direction:

$$\frac{\partial^2}{\partial z^2}E\left(z,t\right)-\frac{1}{c^2}\frac{\partial^2}{\partial t^2}\varepsilon\left(z\right)E\left(z,t\right)=0. \tag{11}$$

The periodic dielectric constant $\varepsilon\left(z\right)$ $(-\infty<z<\infty)$, defined by:

$$\varepsilon\left(z\right)=\begin{cases}\varepsilon_A \text{ if } z \text{ is in } A\\ \varepsilon_B \text{ if } z \text{ is in } B\end{cases}, \tag{12}$$

is expanded into a Fourier series:

$$\varepsilon\left(z\right)=\sum_{p=-\infty}^{\infty}\varepsilon_p e^{i\frac{2\pi p}{a}z}. \tag{13}$$

The basic functions $\left\{e^{i\frac{2\pi p}{a}z}\right\}_{p=-\infty}^{\infty}$ have periodicity of the lattice and the quantity

$$\frac{2\pi p}{a}\qquad(p=0,\pm1,\pm2,...) \tag{14}$$

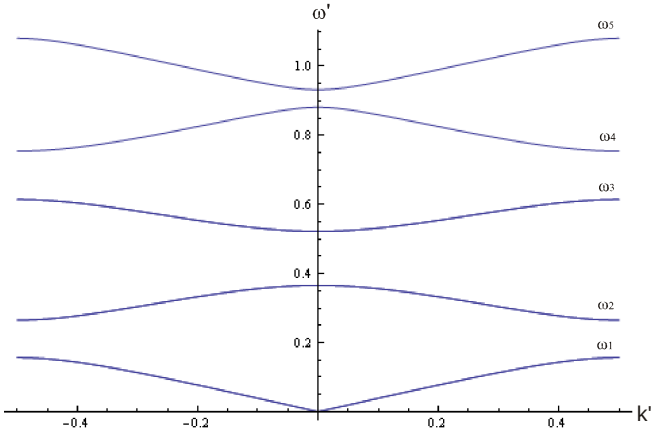

Figure 5: Calculated band structure for 1D photonic crystal using 9 elements in the matrix. The axes are normalized: $\omega' = \frac{\omega a}{2\pi c}$ and $k' = k\frac{2\pi}{a}$. Several bandgaps occur. Only for very small frequencies the dispersion relation approaches straight line as it is in homogeneous material.

defines the reciprocal lattice "vector". We separate the temporal behavior with the use of:

$$E(z,t) = e^{-i\omega t}E(z). \tag{15}$$

To find the solution of the wave equation 11, a Bloch form is assumed for $E(z)$, which is given as:

$$E(z) = \sum_{p=-\infty}^{\infty} c_p e^{i\left(k+\frac{2\pi p}{a}\right)z}. \tag{16}$$

Inserting Eqs. 13 and 16 into Eq. 11 yields:

$$\left(k+\frac{2\pi p}{a}\right)^2 c_p - \frac{\omega^2}{c^2}\sum_{p'=-\infty}^{\infty}\varepsilon_{p-p'}c_{p'} = 0 \qquad (p = 0, \pm1, \pm2, ...). \tag{17}$$

We obtain a system of linear coupled equations for the coefficients $...c_{-1}, c_0, c_1, c_2, ...$ The solution exists only when the determinant of the system is equal to zero:

$$\det\begin{bmatrix} ... & ... & ... & ... & ... \\ ... & \left(k-\frac{2\pi}{a}\right)^2 - \frac{\omega^2}{c^2}\varepsilon_0 & -\frac{\omega^2}{c^2}\varepsilon_{-1} & -\frac{\omega^2}{c^2}\varepsilon_{-2} & ... \\ ... & -\frac{\omega^2}{c^2}\varepsilon_1 & k^2 - \frac{\omega^2}{c^2}\varepsilon_0 & -\frac{\omega^2}{c^2}\varepsilon_{-1} & ... \\ ... & -\frac{\omega^2}{c^2}\varepsilon_2 & -\frac{\omega^2}{c^2}\varepsilon_1 & \left(k+\frac{2\pi}{a}\right)^2 - \frac{\omega^2}{c^2}\varepsilon_0 & ... \\ ... & ... & ... & ... & ... \end{bmatrix} = 0. \tag{18}$$

From Eq. 16 it can be shown, that wave vectors $k \pm \frac{2\pi}{a}p$ all yield the same result as the wave vector k, which implies that all possible solutions (i.e. modes) are covered by letting k having values running only over the first Brillouin zone (BZ), which is for the present 1D system defined by:

$$\frac{-\pi}{a} < k < \frac{\pi}{a}.$$

For a given k in the first BZ the secular equation 18 gives the eigenvalues $\omega_1, \omega_2, ..., \omega_n$, where n is the size of matrix, used in calculations. It can be shown that by increasing n, lower eigenvalues are converging towards the correct value. In Fig. 5 we see that for a single wave vector k, many solutions arise and some of the frequencies are prohibited due to bandgaps.

Analogous to 1D photonic crystals, Maxwell equations yield to the band structure also for 2D microstructures (Fig.6). A PCF is a special case of 2D photonic crystal with a refractive index

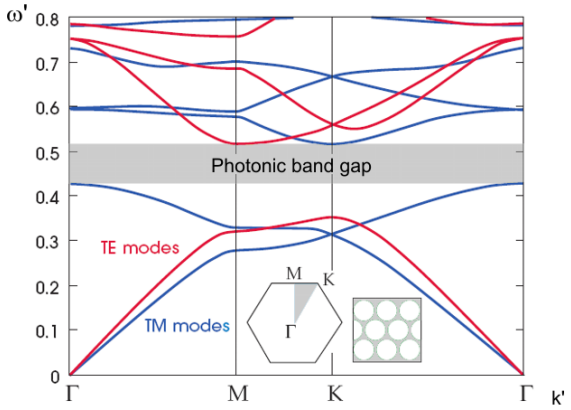

Figure 6: Band structure for 2D photonic crystal with hexagonal lattice. [5].

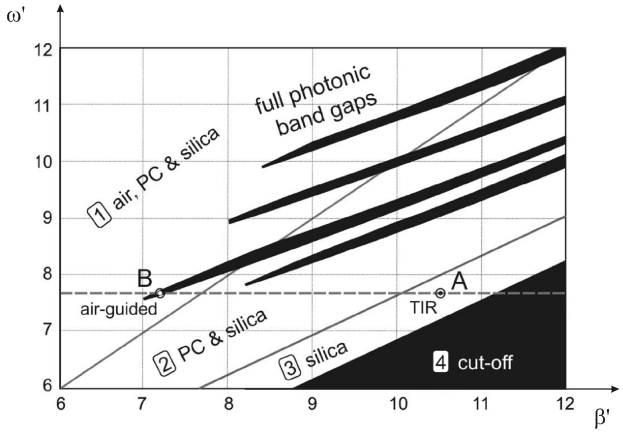

Figure 7: Propagation diagram for a PCF with hexagonal lattice and 45% air-filling fraction. The regions, mentioned on Fig. 2 are still observed: leaky (1), guided (2 and 3) and cutoff (4). Beside standard cuttoff region, additional cutoff "fingers" occur in the guided and leaky regions. For the situation in point B, hollow core guidance is possible. Point A present standard solutions on the principle of total internal reflection on silica-microstructure interface. In region 2, Bloch waves that remain trapped due to the total reflection on air-PCF interface exist. [4]

modulation in xy plane which is elongated in the z direction to obtain a fiber form. To achieve the fiber core, an irregularity in periodic structure is introduced at the center of the microstructure. In the above described simplified calculation of the band structure, we were considering light beams were incident perpendicularly to the layer surfaces. In PCF, light is guided in the core and propagation direction is thus parallel with the index modulating strands, therefore the bandgaps in the $\omega - \beta$ diagram are inclined. In Fig. 7 the propagation diagram of a typical PCF structure with hexagonal lattice and 45% diameter to pitch ratio (d/Λ - the ratio between diameter of air hole d and interhole spacing Λ) is presented. The normalized wave vector β is along the fiber axis. The area can still be divided into the leaky, the guided and the cut-off regions, but on the contrary to classical fibers some bandgap cutoff "fingers" occur in the guided as well as in the leaky region. Inside the bandgaps, above light line for air (point B), light can be trapped in a hollow core and totally reflected from PCF cladding, since no oscillating solution exist in the cladding region and light can't pass the microstructured area. This is one of the most interesting features of photonic crystals: wave guidance can be achieved even if the refractive index of the guiding core material is lower than the index of the cladding which is not possible for standard glass fibers.

4 PCF types

Photonic crystal fibers are fabricated by stacking macroscopic silica tubes in an array, inserting them into larger silica tube and drawing into fiber on draw towers the same way as standard optical fibers. The fabrication process is the same with different array structures; therefore various types of PCFs with specific properties can be produced with a similar effort. In this chapter we will briefly review the known PCF geometries and describe some properties of the most important ones. In Fig. 8 some typical geometry schemes are presented.

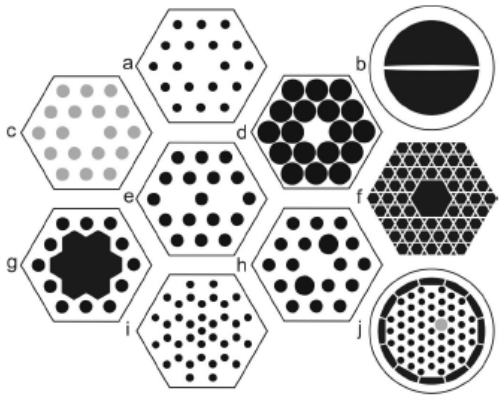

Figure 8: Representative sketches of different types of PCF. The black regions are hollow, the white regions are pure glass and the gray regions are doped glass. (a) Endlessly single mode solid-core (b) Nanoweb fiber (not a PCF). (c) All-solid glass PCF with raised - index doped glass strands (colored gray) in the cladding. (d) solid-core PCF with high air-filling fraction and small core. (e) Dual-core PCF (f) Kagomé hollow core PCF. (g) Seven-cell hollow-core PCF. (h) Birefringent PCF (i) Carbon-ring structure for PBG guidance. (j). Double-clad PCF with offset doped lasing core and high numerical aperture inner cladding for pumping. [4]

4.1 Solid core PCF

The first and still the most common PCF design has the solid core, surrounded by a hexagonal array of air channels (also called "holey" fiber) (Fig. 9). Even though the transverse microstructure in

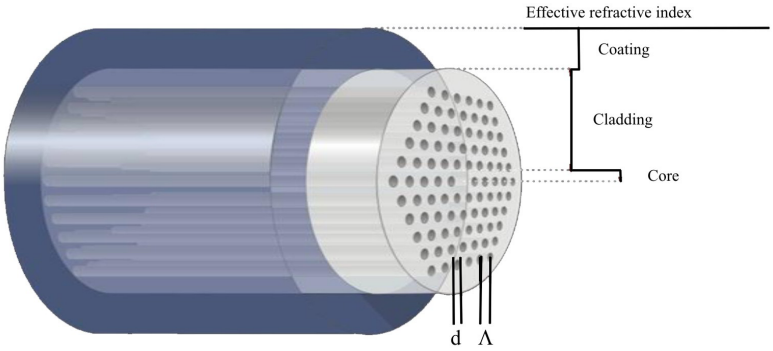

Figure 9: Most common design of PCF with solid core and microstructured cladding. [6]

the cladding imposes quite a complicated band structure, light guidance in solid-core PCF can still be well explained with the total internal reflection of light on the interface between the core which has refractive index of silica and the cladding which has lowered effective refractive index due to air

holes [7]. At long wavelengths, the square of effective index of the cladding is an exact mean value of silica and air indices squared. At shorter wavelengths, the details of microstructure come into play and effective index ratio between the core and the cladding is reduced. According to Eq. 8, lowered index difference imposes shorter wavelength, at which the cut-off relation is fulfilled. Therefore it is possible to design a microstructure configuration in which cut-off condition is always fulfilled and the fiber is "endlessly single mode" (ESM). This means that only the first mode is guided inside the core no matter how short is the wavelength of light [8]. For this condition to be met, the ratio d/Λ should be less than 0.43 [4]. This feature can be understood by considering the array of holes as a modal filter or "sieve". At small values of d/Λ, higher order modes can escape through the glass channels between the holes due to low transverse effective wavelength λ^g_{eff} (corresponding to large transverse wave vector). The fundamental mode has larger transverse effective wavelength and no coupling with outside space through cladding microstructure is possible. According to this feature, it is possible to design very large-area SM core. This allows higher total power to be carried in SM regime due to lower intensity-related nonlinear effects. The ESM feature is one of the most important advantages of solid core PCFs with respect to the standard fibers.

The ZDW of a solid-core PCF depends on the size of the core. Large core fibers ($D > 30\,\mu$m) with d/Λ ratio of 0.43 will have ZDW close to that of silica ($\approx 1.3\ \mu$m). With decreasing D, ZDW also decreases, yielding to approx. 800 nm at $D = 2\ \mu$m [9]. By careful design, ZDW can even be shifted in the visible area. Tailoring dispersion with design is an important feature of PCFs and gives rise to various applications in non-linear optics.

The attenuation of light in solid core PCF is based on two mechanisms: Bulk silica loss and scattering loss related to the roughness at air-glass interfaces. The lowest loss achieved to date is 0.28 dB/km at 1550 nm [10], which is not far from 0.19 dB/km, which is the lowest value in standard SM fiber.

4.2 Hollow core fiber

On the contrary to solid core PCF, hollow core (HC) fibers guide light by a true photonic bandgap. A correctly designed and manufactured HC fiber does not allow light propagation in the microstructured fiber cladding (point B in Fig 7). Since there is no successful coupling between the core and the cladding, light of appropriate wavelength is totally reflected at all angles and is therefore restricted to the region inside the air core. For hollow core guidance, typically the values of d/Λ

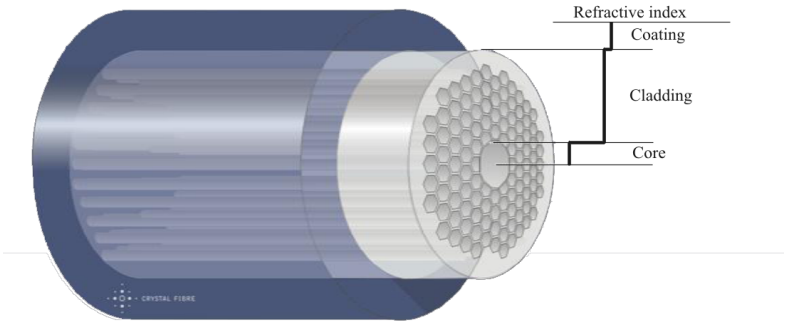

Figure 10: Schematics of holow core PCF. [6]

above 0.9 as well as larger core diameters are necessary. The GVD in HC PCF is decreasing with wavelength, passing zero at ZDW close to the upper bandgap edge and can therefore be adjusted to the application. Attenuation in HC PCF is a promising parameter, since light has very small overlap with silica. It was shown that eight rings of air holes yield transmission losses due to tunneling that are below 0.01dB/km [11]. However, to date best achieved attenuation in HC PCF is 1.2 dB/km which is still significantly worse than in standard solid core fibers [12]. This is

due to the fact, that major attenuation mechanism in HC PCF is not the loss in bulk silica, but scattering on surface oscillations at air-silica interface. This is a direct consequence of fabrication process and so far no easy solutions were found [13]. However, air guidance benefits drastically from the small non-linear refractive index, which determines detrimental nonlinear effects, such as four-wave mixing, self-phase modulation, stimulated Raman scattering etc. The nonlinear index is defined through relation:

$$n = n_0 + n_2 I, \tag{19}$$

where n is overall refractive index, n_0 linear refractive index and I intensity of the beam (in W/m^2). Typical values of n are 2.5×10^{-20} $\mathrm{m^2\,W^{-1}}$ and 2.9×10^{-23} $\mathrm{m^2\,W^{-1}}$ for silica and air, respectively. Due to low overlap of light with glass, an effective nonlinear index of HC PCF can be drastically lower than in silica fibers. The reported values are 8.6×10^{-23} $\mathrm{m^2\,W^{-1}}$ [14]. On the other hand, highly nonlinear behavior can be an advantage for applications based on nonlinear processes. Conversely to HC, very high effective nonlinear indices (as much as 20 times larger than in bulk silica) can be achieved in solid-core PCF, which is beneficial for super-continuum generation, parametric amplification, soliton formation, etc.

Another promising feature of hollow core fibers is the possibility of filling the core region with various gasses or liquids, i.e. creating photonic microcells [15]. Tight and efficient coupling of light to gaseous or liquid material has numerous benefits and various applications are emerging [16].

4.3 Air-clad active PCF

The important PCF design is the air-clad active large-mode area fiber, which is a PCF-alternative to active double-clad fiber. Such fibers are nowadays used to create low cost laser systems with several benefits in comparison with standard lasers. A fast and comprehensive reading about fiber lasers can be found in [17].

The active core, doped with rare earth elements, such as Yb or Er, is surrounded by the air-silica microstructure, which confines signal light to the core. The possibility of large mode area design is beneficial for optical amplification effects, while it still maintains a desired SM operation, yielding high quality profile of the laser light. The pump light is introduced into the inner cladding and is confined by a thin layer of the secondary air cladding (Fig 11). Such a design yields high NA for

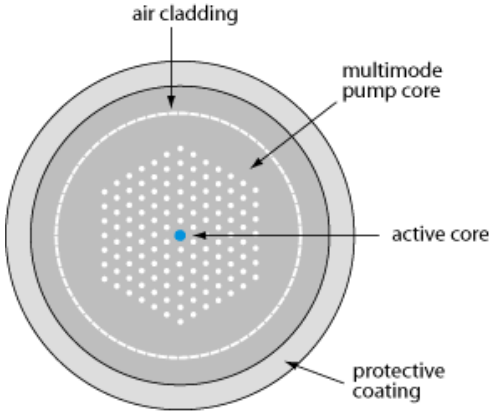

Figure 11: Structure of a photonic crystal fiber with an air cladding. [17]

the pump light (values up to 0.6), which is only limited by practical fiber handling and mechanical stability. High NA gives possibility for the use of low-cost large area pump diodes[1]. In order to reduce non-linear effects, an active fiber must be as short as possible and improved thermal properties are required. Instead of thermally instable polymer coatings, large silica protection

[1]It is known that the product of NA and the beam diameter w remains constant in any optic system. Large area sources can thus be collimated into a small spot for the price of increasing NA.

layers can be used. Using LMA air-clad PCF, the output powers beyond 1 kW have been achieved in a single fiber laser [9].

4.4 Other types of PCF designs

Many different types of PCF structures are possible and each of them has its own specific properties. Polarization maintaining fibers and polarizing fibers are well known by their functionality and can both be achieved by imposing two diametral defects into the cladding microstructure (Fig. 8 h).

Multicore PCFs (Fig 8 e) can be designed with the same effort as with ordinary PCF. The coupling strength between the cores depends on the sites chosen. Applications include curvature sensing and pump light coupling in fiber lasers.

Another interesting design is Kagomé lattice (Fig 8 f) which doesn't support band gaps, but light guidance is achieved in hollow core due to strongly reduced density of states in the cladding [4].

5 Applications

Due to large variety of adjustable parameters, like numerical aperture, dispersion, attenuation, birefringence, non-linear index, the number of modes, etc., which are determined solely by the geometry of PCF, many interesting fiber structures can be fabricated with similar fabrication effort. However, PCF applications are still on the scale of laboratory devices, mainly for the purpose of research and development and mass commercialization have yet to come. We will point out some application aspects regarding high power fiber lasers, as one of the most prominent area for application of PCF technology, and some aspects regarding the use of PCF in telecommunications, being the largest optical fiber industry by far. Besides this, PCFs are very promising in non-linear optics for generation of white light of high spatial coherence (i.e. supercontinuum), parametric amplification and oscillation, correlated photon-pair formation and many other purposes. PCFs can also be used in sensory systems and laser tweezers applications.

5.1 High power PCF lasers

One of the major benefits of fiber lasers in comparison with bulk lasers is the quality of beam, which is close to diffraction limit. Fiber lasers are also immune to thermal lensing and other thermo-optical problems. However, the high intensity of light gives rise to non-linear effects, which are proportional to interaction length and inversely proportional to mode area. In standard glass fibers, large–mode-area double-clad fibers with irregular shape of inner cladding were designed. Low quality pump light is introduced to multimode inner cladding (acting as a waveguide for pump light) and coupled to large-area-core with higher refractive index. To retain single mode operation in such configuration output (and therefore good beam quality), very low NA is required, which makes fibers excessively sensitive to bending. By using air-clad active PCF, significant increase of interaction area is possible, due to ESM behavior. So far single mode spot size up to 60 μm was achieved in PCF [18], which is a great improvement according to 25 μm in best glass LMA DC fibers.

High quality of output beam is needed for efficient beam combining, which results in very high output powers needed for industrial applications. Special photonic crystal beam combiners based on tapered PCFs were designed in order to couple light from several active fibers into one PCF (Fig. 12).

By using air clad PCF, continuous wave (CW) powers of 2.5 kW were demonstrated, which is in the same range as 3 kW achieved by best standard glass LMA DC fiber [19]. However, the beam from PCF is better for beam combining and by using tapered design, output lase powers up to 20 kW in continuous wave (CW) operation mode are possible before the intensity related problems in bulk silica start to appear [6]. The most critical effect is stimulated Raman scattering,

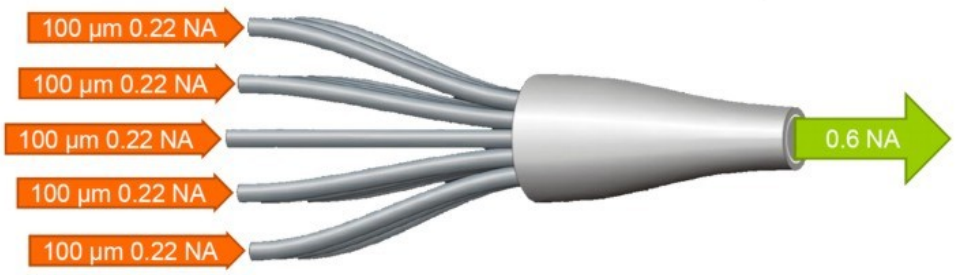

Figure 12: Schematics of PCF beam combiner for high power applications. [6]

but with careful design restrictions related to this effect come close to the limit of thermal stability of bulk silica.

In pulsed regimes, pulse energies up to mJ can be achieved in active PCFs, which is comparable to pulse energy attained in standard glass designs [20]. It is also believed that hollow core PCF, with its superior power handling and designable GVD, is ideal for the last compression stage in chirped-pulse amplification schemes [4].

5.2 PCFs in telecommunications

There are many potential applications of PCFs or PCF-based devices in telecommunications, but, whether these will be adopted, remains an open question. The main advantage of using solid core PCFs in telecom networks lies in its low bend loss, therefore it is well suited for fiber-to-the home applications. However, main disadvantage is at the moment the price, which is still many times higher than that of the standard fiber (100 €/m against 0.4 €/m according to Thorlabs inc.). Another disadvantage can be seen in more demanding fiber handling and lowered mechanical stability. Due to the possibility of accurately tailoring dispersion properties, PCFs could be useful as dispersion-compensating fibers. Yet other options are the use of HC PCF, filled with appropriate gas, for frequency stabilization or possible use of nonlinear properties of PCFs to generate supercontinuum as a source for WDM (wavelength division multiplexing) channels.

Hollow-core PCFs show specific advantages to standard fibers in long-haul telecommunications. The much lower non-linear effects provide the possibility that more overall power can be transmitted and WDM channels can be much more tightly packed without crosstalk. However there are still important weaknesses regarding attenuation and some other detrimental effects (e.g. polarization mode dispersion).

6 Conclusions

Photonic crystal fibers are innovative technology based on the specific behavior of light in periodic dielectric structures. Basic properties of light guidance in PCFs can be understand through simple 1D example, but for deeper insight, advanced numerical simulations must be performed. Due to bandgaps, light guidance in media with lower refractive index or even in the hollow core is possible. PCFs have numerous interesting features which can be tailored only by geometry of transverse microstructure. These features are being intensively investigated and first applications of PCFs are emerging. The two main designs of PCFs are solid-core PCF, which can be designed as single mode fiber all wavelengths, and hollow-core PCF, in which light is guided due to photonic bandgap in the cladding. PCFs are promising technology for high power fiber lasers and high power light transmission. In telecommunications, PCFs can be used for auxiliary devices, whilst for usual waveguides, the attenuation at telecom frequencies must still be reduced and the cost effectiveness on the market must be achieved.

References

[1] J. C. Knight, T. A. Birks, D. M. Atkin and P. At. J. Russel, "Pure silica single-mode fibre with hexagonal photonic crystal cladding", Proc. OFC, PD3, (1996)

[2] A. Yariv, P. Yeh, "Photonics - Optical electronic in modern communications, sixth edition", Oxford university press, 2007

[3] K. Inoue, K. Ohtaka, "Photonic Crystals - Physics, Fabrication and Applications", Springer, 2004

[4] P.St.J. Russel, "Photonic-Crystal Fibers", J. Lightw. Technol. vol. 24, no. 12, pp. 4729-4749, (2006)

[5] J.D. Joannopoulos, S.G. Johnson, J.N. Winn, R.D. Meade, "Photonic Crystals Molding the Flow of Light", Princeton University press, 2008 (available at http://ab-initio.mit.edu/book/photonic-crystals-book.pdf, 29.5.2009)

[6] J. Broeng, "Photonic crystal fibers", in APOC (Hangzhou, 2008).

[7] J. C. Knight, T. A. Birks, P. St. J. Russell, and J. P. de Sandro, "Properties of photonic crystal fiber and the effective index model," J. Opt. Soc. Am. A 15, 748-752 (1998)

[8] T.A. Birks, J.C. Knight and P.St.J. Russel, "Endlessly single-mode photonic crystal fiber", Opt. Lett, vol. 22, no.13, pp. 961-963,Jul. 1997

[9] R. E. Kristiansen, K. P. Hansen, J. Broeng, P. M. W. Skovgaard, M. D. Nielsen, A. Petersson, T. P. Hansen, B. Mangan, C. Jakobsen and H. R. Simonsen, "Microstructured fibers and their applications", OPTOEL '05, pp. 37-42

[10] K. Kurokawa, K. Tajima, K. Tsujikava and K. Nakajima, "Penalty-free dispersion-managed soliton transmission over a 100-km low-loss PCF", J. Lightw. Technl., vol. 24, no.1, pp.32.37, Jan 2006.

[11] X. Yong and A. Yariv, "Loss analysis of air-core photonic crystal fibers", Opt. Lett. 28, 1885-1887 (2003)

[12] P. J. Roberts, F. Couny, H. Sabert, B. J. Mangan, D.P. Williams, L. Farr, M.W. Mason, A. Tomlinson, T.A. Birks, J.C. Knight nd P. St. J. Russel, "Ultimate low loss of hollow - core photonic crystal fibers", Opt. Express, vol 13, no. 1, pp. 236-244, 2005.

[13] T.A. Birks, P.J. ROberts, F. County, H. Sabert, B.J. Mangan, D.P. Williams, L. Farr, M.W. Mason, A. Tomlinson, J.C. Knight, P.St.J. Russell, "The fundamental limits to the attenuation of hollow-core photonic crystal fibres", Proc. of 2005 7th International Conference, vol. 1, pp 105-110. July 2005.

[14] F. Luan, J.C. Knight, P.St. J. Russel, S. Campbell, D. Xiao, D. T. Reid, B.J. Mangan, D.P. Williams and P. J. Roberts, "Femto-second soliton pulse delivery at 800nm wavelength in hollow-core photonic bandgap fibers"m Opt. Express, vol. 12, no. 5, pp. 835-840, Mar. 2004.

[15] F. BEnabid, F. Couny, J.C. Knight, T. A. Birks and P. St. J. Russell, "Compact, stable and efficient all-fibre gas cells using hollow - core photonic crystal fibres", Nature 434, pp. 488-491 (2005)

[16] F. Benabid, P. J. Roberts, F. Couny, P. S. Light, "Light and gas confinement in hollow-core photonic crystal fibre based photonic microcells", J. of European Opt. Soc., Rapid publications 4, 09004 (2009)

[17] R. Paschotta, "Encyclopedia of Laser Physics and Technology", http://www.rp-photonics.com/encyclopedia.html, 31.5.2009

[18] J. Limpert, O. Schmidt, J. Rothhardt, F. Röser, T. Schreiber, A. Tünnermann, S. Ermeneux, P. Yvernault, and F. Salin, "Extended single-mode photonic crystal fiber lasers," Opt. Express 14, 2715-2720 (2006)

[19] V. Fomin, A. Mashkin, M. Abramov, A. Ferin, V. Gapontsev, and IPG Laser GmbH Burbach Germany, "3 kW Yb fibre lasers with a single-mode output," in International Symposium on High-Power Fiber Lasers and their Applications (St. Petersburg, 2006)

[20] O. Schmidt, J. Rothhardt, F. Röser, S. Linke, T. Schreiber, K. Rademaker, J. Limpert, S. Ermeneux, P.Yvernault, F. Salin, and A. Tünnermann, "Millijoule pulse energy Q-switched short-length fiber laser," Opt. Lett. 32, 1551-1553 (2007)